International Journal of Applied Earth Observation and Geoinformation 40 (2015) 100–108

Contents lists available at ScienceDirect

International Journal of Applied Earth Observation and Geoinformation

journal homepage: www.elsevier.com/locate/jag

Regional assessment of lake ecological states using Landsat: A classification scheme for alkaline–saline, flamingo lakes in the East African Rift Valley

E.J. Tebbs[a,d,*], J.J. Remedios[a], S.T. Avery[c], C.S. Rowland[d], D.M. Harper[b,c]

[a] University of Leicester, Department of Physics and Astronomy, University Road, Leicester LE1 7RH, United Kingdom
[b] University of Leicester, Department of Biology, University Road, Leicester LE1 7RH, United Kingdom
[c] University of Leicester, Centre for Landscape & Climate Research, University Road, Leicester LE1 7RH, United Kingdom
[d] Centre for Ecology and Hydrology, Lancaster Environment Centre Library Avenue, Bailrigg, Lancaster LA1 4AP, United Kingdom

ARTICLE INFO

Article history:
Received 17 November 2014
Accepted 23 March 2015
Available online 24 April 2015

Keywords:
Landsat
Classification
Alkaline–saline lakes
Lesser Flamingos
Cyanobacteria
Benthic diatoms

ABSTRACT

In situ reflectance measurements and Landsat satellite imagery were combined to develop an optical classification scheme for alkaline–saline lakes in the Eastern Rift Valley. The classification allows the ecological state and consequent value, in this case to Lesser Flamingos, to be determined using Landsat satellite imagery. Lesser Flamingos depend on a network of 15 alkaline–saline lakes in East African Rift Valley, where they feed by filtering cyanobacteria and benthic diatoms from the lakes' waters. The classification developed here was based on a decision tree which used the reflectance in Landsat ETM+ bands 2–4 to assign one of six classes: low phytoplankton biomass; suspended sediment-dominated; microphytobenthos; high cyanobacterial biomass; cyanobacterial scum and bleached cyanobacterial scum. The classification accuracy was 77% when verified against *in situ* measurements. Classified imagery and timeseries were produced for selected lakes, which show the different ecological behaviours of these complex systems. The results have highlighted the importance to flamingos of the food resources offered by the extremely remote Lake Logipi. This study has demonstrated the potential of high spatial resolution, low spectral resolution sensors for providing ecologically valuable information at a regional scale, for alkaline–saline lakes and similar hypereutrophic inland waters.

1. Introduction

High spatial resolution satellite sensors, such as Landsat, can be used for quantitative monitoring of water quality parameters in small inland waters (Brezonik et al., 2005; Vincent et al., 2004). Due to the broad spectral bands of these sensors, the algorithms employed are typically empirical and require tuning for each water body. This study explored an alternative approach which used the shape of the water-leaving reflectance to classify the ecological states of lakes at a regional scale. This approach was applied to alkaline–saline (soda) lakes in the East African Rift Valley. These lakes support dense blooms of cyanobacteria and extensive areas of microphytobenthos which are important food sources for Lesser Flamingos (Tuite, 2000). In East Africa, the flamingos' survival depends on the food availability throughout a network of 15 alkaline–saline lakes within the Eastern Rift (Childress et al., 2008). Limited *in situ* data are available for these lakes due to their remoteness; hence, remote sensing has potential as an alternative method for monitoring.

Alkaline–saline lakes undergo large fluctuations in water levels that impact strongly on primary producers (Smol and Stoermer, 2010) and the capacity of these lakes to support Lesser Flamingos. At high levels, the shallower lakes can be relatively fresh and support single celled cyanobacterial phytoplankton, which are too small to be filtered by flamingos (Vareschi, 1978), while at intermediate levels they support dense blooms of filamentous cyanobacteria (primarily *Arthrospia fusiformis*; several hundred μg l^{-1}; Oduor and Schagerl, 2007b) which provide a rich supply of food for the flamingos (Vareschi, 1978). Finally, when shallow, the lakes support microphytobenthos, providing a secondary food source for the flamingos (Tuite, 2000). Hence, in terms of value to Lesser Flamingos, the lakes can exist in different states. Often multiple states can occur within a single lake in different areas.

* Corresponding author at: Centre for Ecology and Hydrology, Lancaster Environment Centre Library Avenue, Bailrigg, Lancaster LA1 4AP, United Kingdom. Tel.: +44 01524 595858; fax: +44 01524 61536.
E-mail addresses: emmbbs@ceh.ac.uk, emma.tebbs@gmail.com (E.J. Tebbs), jjr8@le.ac.uk (J.J. Remedios), sean@watres.com (S.T. Avery), clro@ceh.ac.uk (C.S. Rowland), dmh@le.ac.uk (D.M. Harper).

http://dx.doi.org/10.1016/j.jag.2015.03.010
0303-2434/

Water-leaving reflectance spectra contain information about the optically-active water constituents (Kirk, 1994), and hence, these signals can be exploited in order to infer lake ecological states. Previous studies have classified natural waters in terms of their optical properties (Jerlov, 1976; Case I/Case II, Morel and Prieur, 1977), including the shape of the water-leaving reflectance spectra (Lobo et al., 2012; Kutser et al., 2006; Kurekin et al., 2014). Reflectance-based classifications have been used to inform algorithm selection prior to water quality parameter retrieval (Li et al., 2012; Sun et al., 2012; Shi et al., 2013; Liu et al., 2013). For hypereutrophic lakes, the red and NIR bands of multispectral sensors have been used to classify trophic status, by utilising the strong NIR peak which is characteristic of these waters (Matthews et al., 2012; Tebbs et al., 2013b).

A site-specific algorithm exists for quantifying cyanobacterial biomass in Lake Bogoria, a key feeding lake for the flamingos (Tebbs et al., 2013b). However, the development of generic or customised algorithms for quantifying primary producers in all soda lakes would be extremely challenging, due to their optical complexity and a lack of sufficient *in situ* data. Hence, an alternative approach was taken, to classify the functional states of the lakes based on their spectral signatures. *In situ* data for selected alkaline–saline lakes was used to determine the spectral characteristics of the different ecological conditions and to develop a Landsat-based optical classification. *In situ* reflectance and water parameter measurements were used to define five reference classes for development and validation of the classification scheme. Examination of Landsat imagery identified additional water types not represented by the *in situ* data and this information was also used to inform the classification scheme development. The classification was applied to produce maps and timeseries for several Eastern Rift Valley lakes, showing the spatial and temporal distribution of the different ecological states and the Lesser Flamingo's food supply.

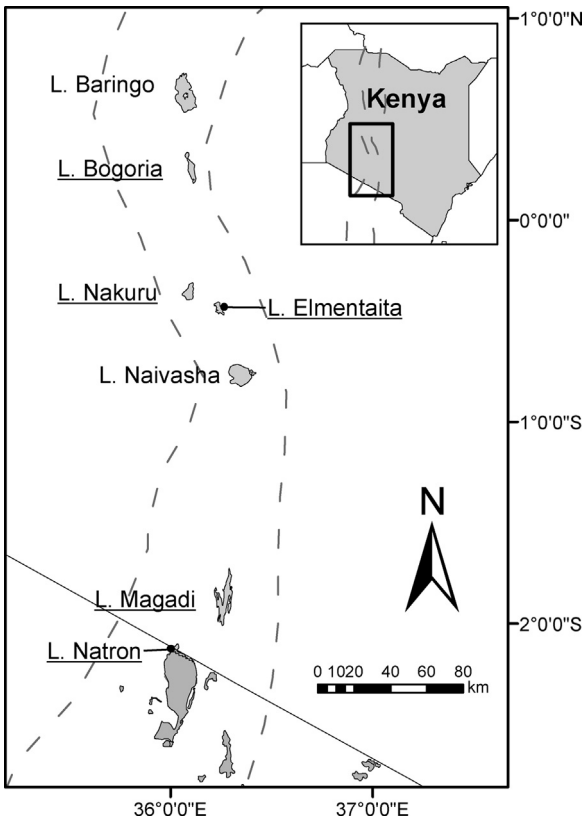

Fig. 1. Map showing locations of the lakes within the East African Rift Valley. Underlined lakes are alkaline–saline, the others are fresh. Lake Oloidien (not shown) is a bay in the SW corner of Lake Naivasha which becomes separated at low water levels. The solid line shows the border between Kenya and Tanzania, the dotted line shows the boundary of the Rift Valley.

2. Study sites

In situ spectral reflectance and water parameter measurements were made at alkaline–saline lakes in Kenya and Tanzania, including Bogoria, Elmenteita, Nakuru, Natron and Oloidien (Fig. 1 and Table 1). These lakes are representative of the range of conditions found in soda lakes: Bogoria and Oloidien are relatively deep and support dense cyanobacterial blooms, while Elmenteita and Natron are shallow, typically supporting benthic diatoms, and Nakuru has an intermediate water level.

3. Method

3.1. In situ reflectance and water parameter measurements

Reflectance and water parameter measurements were collected at the study lakes between 2010 and 2012. At lakes Bogoria, Nakuru and Oliodien, spectral measurements were made from a boat using a GER1500 spectroradiometer. Water samples were collected and analysed for chlorophyll-a (Chl-a), absorption by coloured dissolved organic matter at 440 nm ($a_{CDOM}(440)$), total suspended solids (TSS) and inorganic suspended solids (ISS). Secchi disk depth was also recorded. At Lake Elmenteita and the shallow northern lagoon at Lake Natron the reflectance of algal communities on bottom sediments was measured using a GER1500 mounted on a tripod. Samples of benthic microbial communities were collected using a Gilson corer. Samples of the overlying water were also collected and analysed for Chl-a, a_{CDOM}, TSS and ISS.

When collecting spectoradiometric data, a nadir viewing geometry was used and upwelling radiance was measured between 400 nm and 950 nm. A reference scan of a calibrated Spectralon reference panel was made between each measurement and was used to convert absolute reflectance during post-processing (Robinson and Arthur, 2012). The response of Landsat ETM+ was simulated by convolution of the *in situ* spectra and the spectral response function of each band (Irish, 2000). Chl-a was extracted in 90% acetone after gentle vacuum filtration and followed by manual grinding of the filter paper. Using a spectrophotometer, the absorbance at 663 nm and 750 nm was measured and the Chl-a concentration was calculated (Talling and Driver, 1963). Full details of the procedures used for water parameter and spectral measurements can be found in Tebbs et al. (2013b) and Tebbs (2014).

3.2. Landsat ETM+ satellite imagery

Landsat ETM+ images for the lakes were downloaded from the USGS Global Visualization Viewer, http://glovis.usgs.gov/, for the period 1999–2012. The images were processed using ENVI+IDL software. Radiometric calibration to top-of-atmosphere radiance, L_{TOA}, was performed (Chander et al., 2009). After May 2003 the Scan Line Corrector on Landsat 7 failed and, as a result, affected ETM+ images contain lines of missing data. These gaps were filled using simple spatial linear interpolation.

3.3. Development of the classification

A decision tree (DT) based classification was developed by combining insights gained from *in situ* measurements and satellite image interpretation with knowledge from the literature. *In situ* spectral and water parameter measurements were used to define a set of five classes, 'Low biomass', 'Sediment', 'Scum',

Table 1
Summary of the alkaline–saline lakes sampled in this study.

Lake	Location	Depth (m)	Max area (km^2)	Ecology	References
Bogoria	0°15′ N 36°06′ E	10–12	34	Can support up to 1 million flamingos feeding on dense *A. fusiformis* blooms.	Harper et al. (2003)
Nakuru	0°22′ S 36°05′ E	4.5	40	Shifts between state depending on lake level. At times it has supported most of the East African Lesser Flamingo population, subsisting on *A. fusiformis* blooms.	Vareschi (1978)
Elmenteita	0°27′ S 36°15′ E	3	20	Undergoes rapid changes in primary producers associated with level changes. Epipelic diatoms typically dominate.	Melack (1988)
Oloidien	0°48′ S 36°156′ E	6	6	A bay of freshwater Lake Naivasha at times of high water levels; when separated, its salinity progressively increases, and it begins to support *A. fusiformis*.	Harper and Mwinami (2006)
Natron	02°25′ S 36°00′ E	<3	804	Sole breeding site for Lesser Flamingos in East Africa. Feeding takes place in shallow lagoons around the lake margin.	Brown (1971)

'Microphytobenthos' and 'High biomass', which had distinct spectral features that would aid their discrimination in Landsat imagery. Each of the *in situ* measured spectra was assigned to one of these reference classes based on water quality parameter measurements and other *in situ* observations. For most sites the measured Chl-a was used to assign the class ('Low biomass': Chl-a < 100 μg l^{-1}; 'High biomass': 100 < Chl-a < 800 μg l^{-1}; or 'Scum': Chl-a > 800 μg l^{-1}). For sites where Chl-a was not available, visual observations, microscopy and other water parameter measurements were used to infer the class. For further details on the assignment of the reference classes, and for descriptions of the observed hyperspectral reflectance spectra, see Tebbs (2014). The *in situ* spectra re-sampled to Landsat bands were then sorted according to these reference classes and used for classification development and validation. Atmospherically corrected Landsat imagery was used to retrieve spectral information for classes that were not well represented by the *in situ* data. For development of the DT, the reflectance in the visible and NIR bands of Landsat ETM+ were considered. Landsat ETM+ short wave infrared bands were not considered since water-leaving reflectance is negligible at these wavelengths (Shi and Wang, 2009).

3.4. Atmospheric correction

Images were converted to surface reflectance by applying a Dark Object Subtraction - Cosine of the solar zenith angle (DOS-COST) method (Chavez, 1996). The atmospheric path radiance, L_{haze}, was estimate using the method from Chavez (1988):

$$L_{haze,\lambda} = L_{haze,0}(\lambda/\lambda_0)^{-\alpha} \quad (1)$$

where λ and λ_0 are the central wavelengths of the spectral bands and α is the Angström coefficient which describes the wavelength dependence. $L_{haze,0}$ is estimated from the lowest pixel radiance in the starting haze band, assuming a constant level of haze across the image. α was estimated using a regression of $\ln(\lambda/\lambda_0)$ versus $\ln(L_{haze,\lambda}/L_{haze,0})$ for image bands 1–3 (for further details see Tebbs, 2014).

3.5. Production of classified maps and timeseries

The DT was applied to atmospherically corrected Landsat ETM+ imagery to produce classified maps. For each image, the surrounding land surface was masked out using the Modified Normalised Difference Water Index ($MNDWI = (Green - SWIR)/(Green + SWIR)$; Xu, 2006) applied to atmospherically corrected imagery. Timeseries were produced to show variation in the ecological classes present in selected lakes over time.

4. Results

4.1. Limnological conditions

A wide variety of water types were observed at the lakes sampled, as summarised in Table 2.

4.2. Development of an optical classification scheme

4.2.1. Insights gained from in situ data

In situ spectra were re-sampled to Landsat ETM+ bands, sorted according to the reference classes (Fig. 2) and used to identify spectral features characteristic of particular ecological states. The re-sampled *in situ* spectra exhibited a large amount of variability in shape and magnitude (Fig. 2). For low biomass waters, all bands showed very low reflectance with the highest magnitude typically being seen at R_{560} (Fig. 2A). The sediment spectra either peaked at R_{662} or increased in magnitude towards longer wavelengths. The spectra for high cyanobacterial biomass exhibited a peak at R_{560}, a minima at R_{662} and a high reflectance in the NIR band, R_{835}. A similar spectral shape was observed for cyanobacterial scum, but with much higher NIR reflectance. Finally, for sites where microphytobenthos was observed the magnitude increased gradually, from one band to the next, towards longer wavelengths. Hence, the spectral shapes observed for sediment and microphytobenthos were very similar. The key difference was that for microphytobenthos R_{662}/R_{560} was less than R_{835}/R_{662}, due to the Chl-a absorption feature at 670 nm.

4.2.2. Insights gained from examination of Landsat imagery

Examination of the Landsat satellite imagery showed that some classes were poorly represented by or completely absent from the *in situ* dataset.

In September 2004, a collapse of the *A. fusiformis* bloom took place in Lake Bogoria (Oduor and Schagerl, 2007b; Tebbs et al., 2013). It is likely that, at this time, the lake was dominated by the decay products of *A. fusiformis* (Tebbs et al., 2013b). The detritus present in the lake caused the lake spectra to peak at R_{662} (Fig. 3D), giving a spectral shape similar to sediment but with a lower magnitude. Therefore, a R_{835} threshold was added to distinguish these pixels from sediment.

Table 2
Summary of mean water parameter values observed at the study lakes. Water quality parameters are quoted as mean ± standard deviation.

Lake	Dates	Chl-a ($\mu g\ l^{-1}$)	$a_{CDOM}(440)$ (m^{-1})	TSS ($mg\ l^{-1}$)	ISS ($mg\ l^{-1}$)	Secchi (cm)	Dominant primary producers
Bogoria	Apr 2010	901 ± 971	15 ± 3	54 ± 39	10 ± 7	14 ± 5	*A. fusifomis*
	Apr 2012	272 ± 93	–	–	–	35 ± 6	*A. fusiformis* (unhealthy state)
Oloidien	Mar–Apr 2011	265 ± 93	12.3 ± 1.5	59 ± 96	0.007 ± 1	19 ± 4	Filamentous cyanobacteria, either *Anabaenopsis elenkinii* or a small sized ecotype of *A. fusiformis* (V. Robinson pers. com.)
Nakuru	Apr 2012	172 ± 25	–	–	–	22 ± 1	Single celled, non-vacuolate *Synechococcus* (V. Robinson pers. com.)
Elmenteita	Apr 2010	65 ± 72	–	–	–	–	Site 1: *A. fusiformis*; Site 2: benthic diatoms.
	Mar 2011	215 ± 176	14 ± 4	127 ± 82	60 ± 65	20 ± 3	Small diatoms.
Natron northern lagoon	Apr 2011	–	34 ± 5	2300 ± 900	2000 ± 900	–	Microphytobenthos

Areas of bleached scum were identified in true colour imagery of Lake Bogoria, based on their green/white colour and their complex spatial structure. Although bleached scum was not observed at L. Bogoria during this study, it has been observed there on several previous occasions (pers. obs.). Prolonged UV exposure of the surface layer of cells degrades photosynthetic pigments, reducing absorption in the visible, and breaks down cell structure, reducing scattering in the NIR. Hence, these bleached scum areas had a similar spectral shape to low biomass waters but with higher reflectance in all bands, particularly at R_{560} (Fig. 3B). Therefore, a threshold of $R_{560} > 0.65$ was applied to separate bleached scum from areas of low biomass. Areas of advanced bleached scum, which has started to turn brown, were also observed in the imagery. The spectra of these areas peaked at R_{662} (Fig. 3C). An additional rule was added, based on the ratio R_{560}/R_{835}, to separate advanced bleached scum from sediment. Bleached scum and advanced bleached scum were spectrally separable but ecologically they have the same significance so they were grouped together as a single 'bleached scum' class.

4.2.3. Insights gained from the literature

The rule for differentiating scum from other classes was developed using the scum threshold (Chl-a > 800 $\mu g\ l^{-1}$) and the bottom-of-atmosphere reflectance based Chl-a algorithm for Lake Bogoria derived in Tebbs et al. (2013b):

$$\text{Chl-a} = 26 + 190(R_{835}/R_{662})$$

From this it follows that spectra with $R_{835}/R_{662} > 4.07$ should be classed as scum.

4.2.4. Decision tree

Based on these observations a DT was developed (Appendix A, Fig. A.1), which was able to distinguish six classes (Table 3). Each of the rules in the DT has a bio-physical basis.

4.3. Verification of the decision tree

To assess the suitability of the DT the re-sampled *in situ* spectra were classified using the DT. The classification was then verified

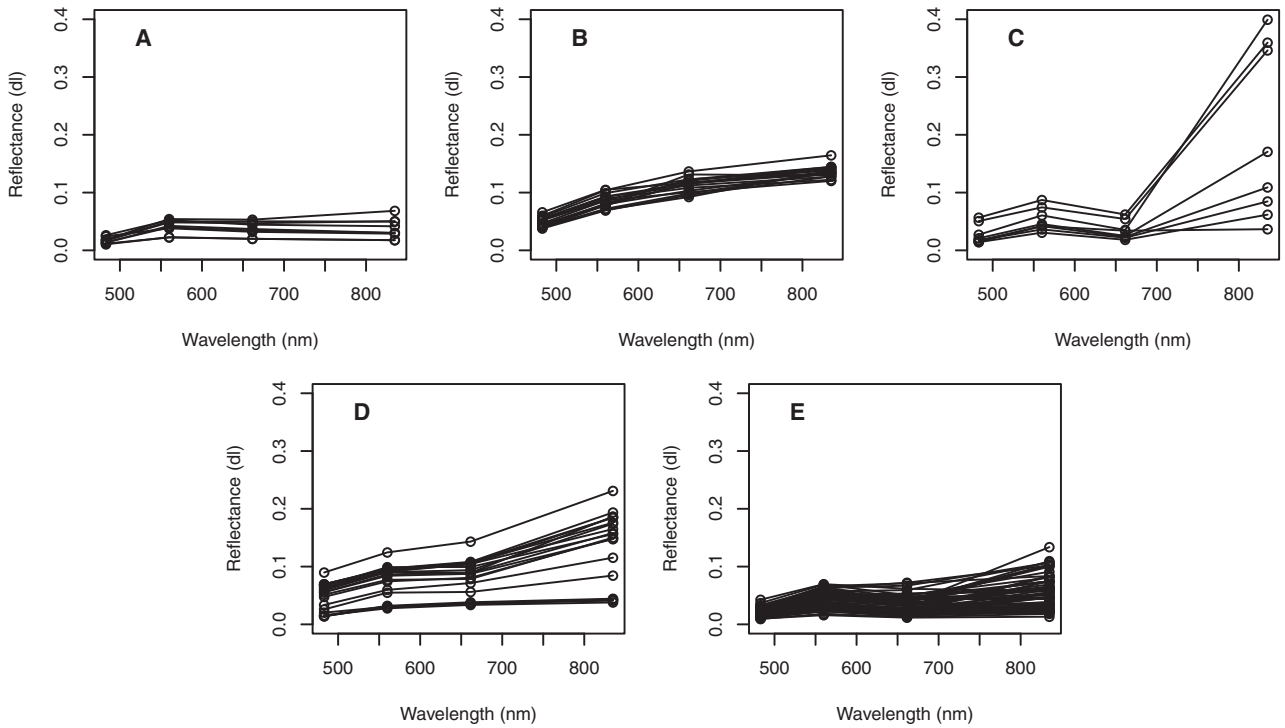

Fig. 2. *In situ* reflectance spectra resampled to Landsat ETM+ bands, sorted into the following classes based on *in situ* water parameter measurements: 'Low biomass' (panel A); 'Sediment' (panel B); 'Scum' (panel C); 'Microphytobenthos' (panel D) and 'High biomass' (panel E).

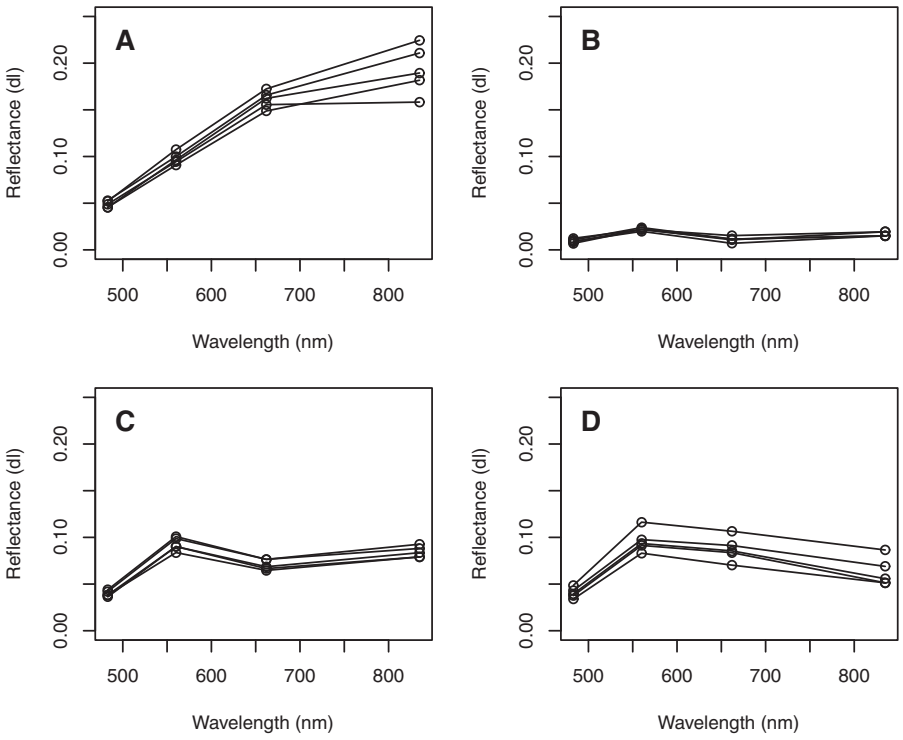

Fig. 3. Reflectance spectra captured from atmospherically corrected Landsat ETM+ imagery for water types not represented by the *in situ* spectral library, including sediment (panel A), bleached scum (panel B), heavily bleached scum (panel C) and detritus (panel D).

by comparing the predicted classes with the reference classes (Table 4). Since no bleached scum was observed *in situ*, initially the verification was carried out using DT shown in Fig. A.1, but with the rule identifying bleached scum left out (initial DT). The overall classification accuracy was 77%. Much of the disagreement between the predicted and reference classes is believed to be due to the difficulties in correctly assigning the reference classes to the *in situ* spectra, as described in Tebbs (2014), rather than failure of the classification scheme.

Verification was also carried out on the final DT, including the rule for distinguishing bleached scum. The addition of this rule had little effect on the classification result, except that the classification of two scum spectra changed to bleached scum.

4.4. Application of the classification scheme to Landsat ETM+ imagery

The DT was used to produce classified maps for lakes where *in situ* measurements were collected, and also for Lake Logipi due to its potential importance to Lesser Flamingos (Fig. 4).

The classified maps of Lake Bogoria agreed extremely well with visual observation of RGB true colour imagery (Fig. 4A). They appeared to accurately delineate areas of scum, bleached scum and sediment. The success of the classification scheme for Bogoria was aided by the relative simplicity of the lake, the existing knowledge of its optical properties (Tebbs et al., 2013b) and local knowledge which was available for identifying the presence of bleached scum in the satellite imagery.

The classified maps for Lake Nakuru gave very good agreement with the RGB imagery (Fig. 4B). The classification picked out areas of cyanobacterial scum and small plumes of sediment and low biomass waters originating from the main river inflows. It also identified bands of microphytobenthos close to the lake edge.

For Lake Elmenteita, most classified maps gave reasonable agreement with the RGB imagery (Fig. 4C). However, on some occasions, when the lake was classed as bleached scum, visual interpretation of the imagery suggested that the lake was actually being influenced by sediment; unlike Lake Bogoria, Elmenteita is shallow, so sediment re-suspension is possible. It is difficult to be certain of this explanation due to a lack of *in situ* knowledge about lake conditions to aid interpretation of the satellite imagery. Elmenteita is highly complex due to its shallow depth and it is more diverse than other alkaline–saline lakes in terms of the phytoplankton communities it supports. Therefore, the *in situ* spectra collected at Elmenteita many not be representative of the range of conditions present in the lake.

Although no *in situ* data from Lake Logipi were available for development of the classification scheme, classified maps of the lake appear very convincing (Fig. 4D). They agree closely with visual

Table 3
Final classification of optical water classes using *in situ* and Landsat data.

Class	Characteristics	Alternative interpretation	Value to flamingos
1	Low biomass	Non-vacuolate phytoplankton or detritus	None
2	Sediment	–	None
3	Scum	–	Low
4	Bleached scum	Sediment	None
5	Microphytobenthos	Mixed sediment and high biomass	Moderate
6	High biomass	–	High

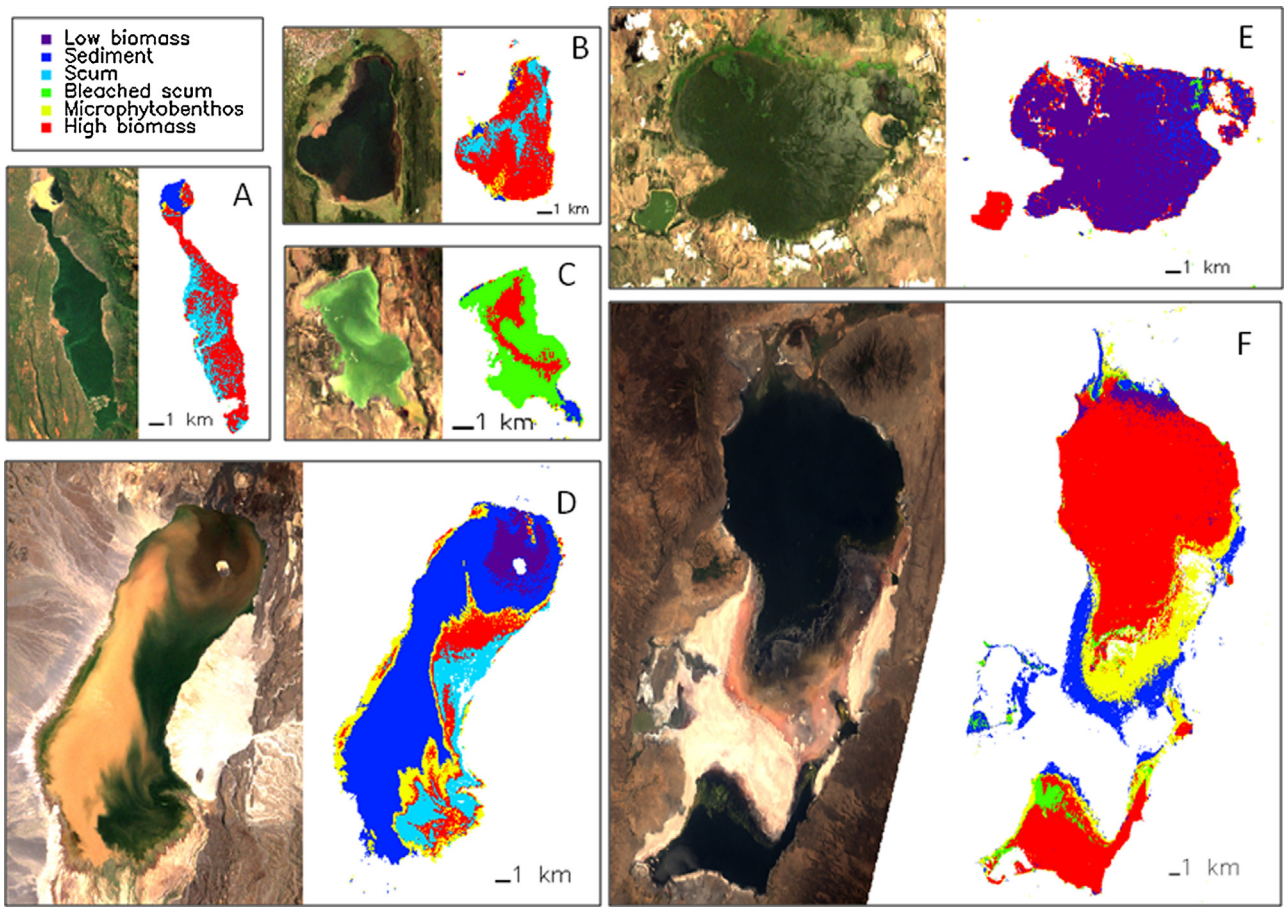

Fig. 4. RGB true colour Landsat ETM+ imagery and classified images for lakes: Bogoria, 2005-05-16 (panel A); Nakuru, 2007-09-11 (panel B); Elmenteita, 2008-08-28 (panel C); Logipi, 2007-08-26 (panel D); Naivasha, 2011-03-30 (panel E); and Natron, 2007-09-27 (panel F). (For interpretation of the references to color in this figure, the reader is referred to the web version of this article.)

interpretations of the RGB imagery and they also agree with the classes that we would expect to find there, predominantly sediment and microphytobenthos.

Classified maps of Lake Oloidien included the adjacent freshwater Lake Naivasha. The maps illustrated the contrast between the two lakes, since Lake Naivasha was classified predominantly as low biomass, while Oloidiens's waters were classed as high cyanobacterial biomass (Fig. 4E). The maps also highlighted that the classification can only reliably be applied to alkaline–saline lakes (which do not support macrophytes) because areas classed as high cyanobacterial biomass for Lake Naivasha were in fact mixed pixels of water and floating vegetation (papyrus and water hyacinth), which are spectrally identical to scum in Landsat bands 1 to 4.

Classified maps of Lake Natron's northern lagoon showed areas of sediment and microphytobenthos, as observed *in situ*, and other lagoons around the lake's margin were classed as either sediment, microphytobenthos or high biomass, as would be expected (Fig. 4F). The uniquely hypersaline brine at the centre of Lake Natron, which typically appears red in Landsat satellite imagery due to extremophile bacteria, was classified as 'High biomass'. Lesser Flamingos cannot feed on this red, single-celled bacteria; therefore, the centre of the lake should be masked out and the classification should only be applied to lagoons around the lake edge, which are kept fresher by inflowing water from springs and rivers.

The classified maps also showed that areas of mixed sediment and high biomass were wrongly classified as microphytobenthos due to their similar spectral shape (Fig. 4A). The lake surface area

Table 4
Confusion matrix for the initial DT. Note that the initial DT did not include class 4 as there was no *in situ* data available for this class.

	Class	Landsat based classification						
		1	2	3	4	5	Total	Accuracy (%)
Reference data	1	**6**	1			2	9	67
	2		**12**		4		16	75
	3			**5**		3	8	63
	4	–	–	–	–	–	–	–
	5		3		**16**	1	20	80
	6	8			6	**55**	69	80
	Total	14	16	5	26	61	122	
	Accuracy (%)	43	75	100	62	90		

The bold values, along the diagonal of the confusion matrix, give the number of correctly classified spectra.

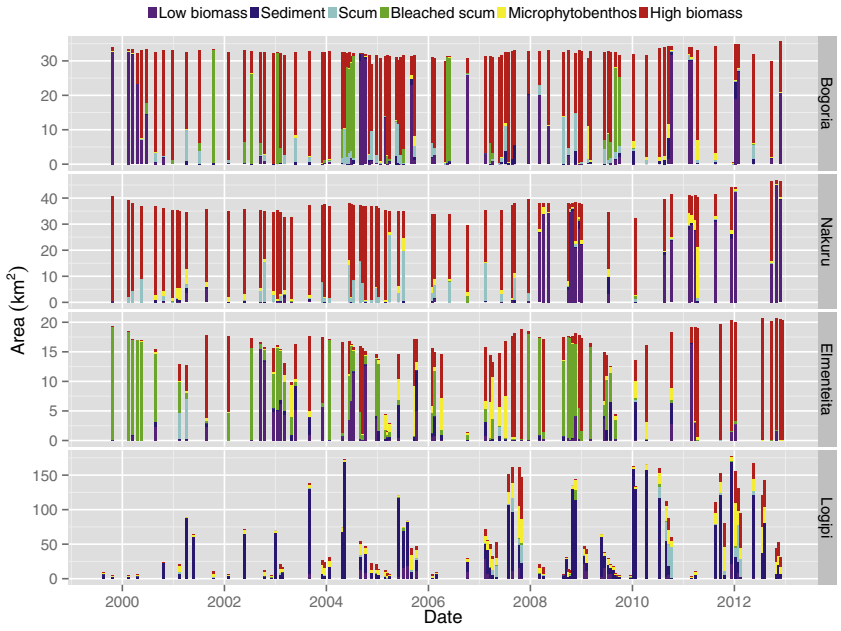

Fig. 5. Timeseries of water types present in lakes Bogoria, Nakuru, Elmenteita and Logipi estimated from Landsat ETM+ imagery. Note the difference in y axis scale between the plots. For a colour version of this figure, the reader is referred to the web version of this article.

mask wrongly categorised the densest areas of cyanobacterial scum as land, but this typically only affected a very small area of the image.

4.5. Timeseries of lake classes

Fig. 5 shows timeseries of water types present in lakes Bogoria, Nakuru, Elmenteita and Logipi (1999–2012).

In Lake Bogoria, high cyanobacterial biomass was the most common class, followed by low biomass and bleached scum, with mean areas of 19.6, 5.8 and 3.9 km^2 respectively. The timeseries showed a gradual transition from low to high biomass from 1999 to 2001, and several episodes of low biomass which correspond to bloom collapse events (Tebbs, 2014). There were periods when most of the lake surface was covered by bleached scum. A particularly prominent episode of bleached scum followed by low biomass was observed in mid 2004, which coincided with a major *A. fusiformis* die-off event (Oduor and Schagerl, 2007a).

In Lake Nakuru, high cyanobacterial biomass was also the most common class, followed by low biomass and cyanobacterial scum (mean areas: 23.6, 8.5 and 3.1 km^2 respectively). Prior to 2008 the lake was dominated by high biomass and scum. In 2008, following rising lake levels throughout 2007, and the occurrence of low cyanobacterial biomass became more common. There was a slight return of high biomass waters in 2010 after decreasing lake levels throughout 2009. The lake then returned to a state of low biomass from the end of 2010 onwards. Throughout the whole class timeseries a very small amount of bleached scum was observed in Lake Nakuru. The results are consistent with Kaggwa et al. (2012) which showed low biomass in Lake Nakuru at the start of 2009.

Lake Elmenteita showed the most variability in the composition of water types present. The lake was dominated by high biomass, but high levels of bleached scum were also present (mean areas: 6.8 and 5.2 km^2 respectively). Between 2000 and 2006 the occurrence of low biomass increased. There was a shift towards high biomass from 2011 onwards. The lake showed two dry periods and one low period.

Lake Logipi showed a high degree of variability in lake surface area, with intermittent flooding and quite regular dry periods. Sediment dominated waters were the most common, followed by microphytobenthos and high biomass waters (mean areas: 36.2, 9.7 and 8.1 km^2 respectively). The lake almost always supported some microphytobenthos and high biomass; out of all the lakes it had the highest average microphytobenthos concentration. The largest areas of high biomass and microphytobenthos were observed in 2007 and from late 2011 to the end of 2012.

5. Discussion

The spectral measurements collected in this study illustrate the wide range of optical water types present in alkaline–saline lakes (Fig. 2). Results showed that it is possible to separate different ecological states based on their spectral signatures. Observations were consistent with previous studies which showed that the magnitude of the reflectance peak in the NIR can be used as an indicator for Chl-a or trophic status (Gitelson, 1992; Matthews et al., 2012). NIR reflectance also contains information about phytoplankton species; vacuolate cyanobacteria have a higher NIR signal than non-vacuolate species (Dubelaar et al., 1987). Therefore the low NIR reflectance observed at Nakuru was a result of both lower biomass and the presence of a singled celled and hence non-vacuolate phytoplankton species. Some papers would refer to the spectral shape classified as low biomass in this study as being characteristic of high biomass waters, however it actually represents the lower end of the biomass range observed in alkaline–saline lakes.

The areas of bleached scum observed in Lake Bogoria were similar to areas of heavily bleached cyanobacterial scum observed as white patches in Landsat imagery at other hypereutrophic lakes (Oberholster and Botha, 2010). The classification scheme was not able to distinguish mixed sediment and high biomass from microphytobenthos in Landsat imagery, due to their similar spectral shape. Fortuitously, the value to flamingos in both cases is moderate.

Lake Bogoria showed episodes of extensive bleached scum coverage while Lake Nakuru had negligible bleached scum, suggesting that Nakuru is more well mixed than Bogoria. Bleached scum is likely to deter flamingos from feeding since they risk clogging clog their filter system. Kaggwa et al. (2012) found that flamingos

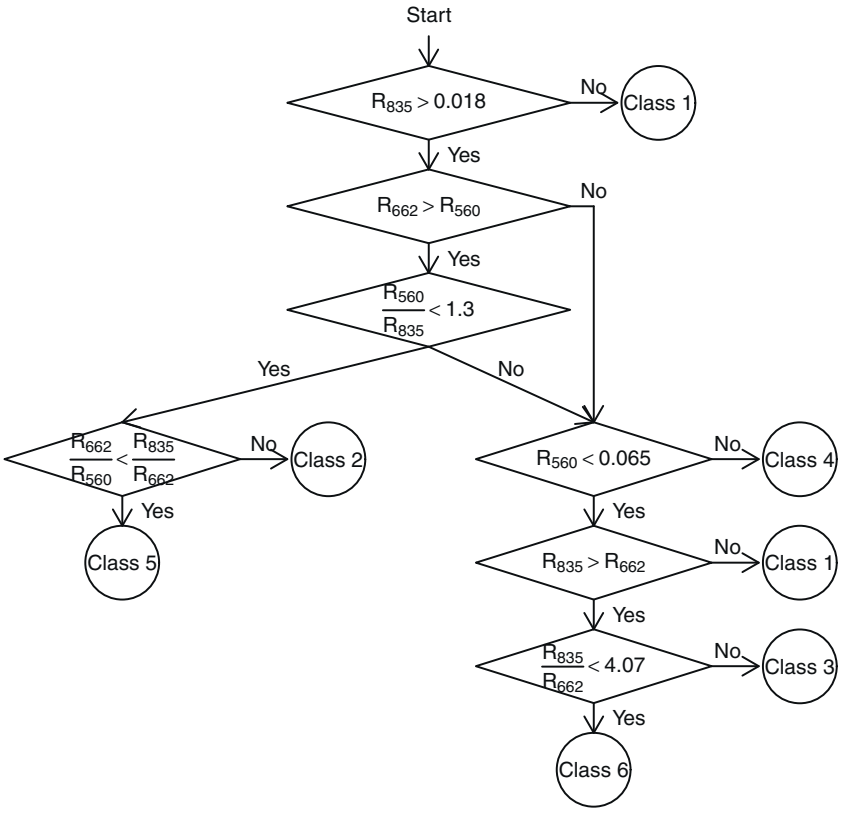

Fig. A.1. Final DT showing how Landsat lake reflectance spectra are classified into one of 6 classes based on the reflectance in each band. Note the initial DT did not include class 4 (bleached scum).

numbers fluctuated at Bogoria throughout 2009 despite a relatively constant *A. fusiformis* biomass. This could be due to the presence of scum in mid 2009 as observed in the class timeseries (Fig. 5). Kaggwa et al. (2012) observed algal mats during their study and suggested this as a potential cause for the observed flamingo deaths. Other studies have suggested that toxins produced by thick cyanobacterial scums have contributed to flamingo deaths (Lugomela et al., 2006).

In Lake Elmenteita, the class timeseries showed a transition from high biomass to low biomass in mid 2004 which agrees with decreasing Chl-a concentrations observed by Oduor and Schagerl (2007b). However, it also suggested that the lake has become more suitable for Lesser Flamingos since 2011, when it moved to a state of high biomass. This is not in agreement with ground observations which suggest that few flamingos have used the lake since 2008 (V. Robinson, pers. comm.). This is further evidence that the results for Elmenteita are less reliable than for the other lakes. It also suggests that the red:NIR threshold for distinguishing between low and high biomass waters may need further tuning.

Logipi showed a high degree of variability in lake surface area, in agreement with observations by Castanier et al. (1993). The class timeseries showed that Lake Logipi was most suitable for Lesser Flamingos from 2007 to early 2008 and from late 2011 to the end of 2012, the latter is significant because at this time, due to high lake levels, Oloidien, Elmenteita and Nakuru did not support significant numbers of flamingos. 3/4 of a million were at L. Bogoria and the authors of this paper initially hypothesised that the rest of the E. African population could have been at Lake Logipi. Our results support this hypothesis by suggesting that Logipi would have been able to support significant numbers of flamingos at this time.

Similar classification schemes for lakes could be developed using MERIS, and the planned Ocean and Land Cover Instrument (OLCI) on Sentinel-3, to improve the classification capability by allowing finer spectral features to be sampled. The classification could also be adapted for the planned Multi Spectral Instrument (MSI) on Sentinel-2, allowing information on lake ecological state to be captured with both high spatial and high temporal resolution. The robustness of the classification could be improved with additional *in situ* measurements, particularly for under-represented water types such as bleached scum and highly variable lakes such as Elmenteita. The authors will extend this work in future by applying the classification to all lakes in the flamingos' key site network, in order to assess the spatial and temporal variability of the Lesser Flamingos' food supply throughout the whole Eastern Rift Valley.

6. Conclusion

This study has demonstrated the potential of high spatial resolution, low spectral resolution sensors for providing ecologically valuable information at a regional scale, for alkaline–saline lakes and similar hypereutrophic inland waters. A Landsat-based optical classification was developed which was able to distinguish five classes ('Low biomass', 'Sediment', 'Scum', 'Microphytobenthos' and 'High biomass') with an overall classification accuracy of 77% when verified against *in situ* measurements. Examination of the Landsat ETM+ imagery showed the presence of an additional water type, 'Bleached scum', which was not represented in the *in situ* dataset, and the classification was modified accordingly. Classified maps and timeseries have demonstrated the differences between alkaline–saline lakes in terms of the water types present. The results have highlighted the importance to Lesser Flamingos of Lake Logipi. Significant food resources were present in the lake at times when feeding conditions were poor at the flamingos other main feeding lakes. This is an important result because

Lake Logipi is difficult to monitor *in situ* due to its extreme remoteness.

Acknowledgements

The authors would like to thank the following people and organisations: the Centre of Interdisciplinary Science, University of Leicester, for funding the PhD study which produced this work; the NERC Field Spectroscopy Facility for providing field equipment and training; Victoria J. Robinson for providing information on primary producers; camp staff in Kenya including camp manager Velia Carn, cooks Willy and Patrick, drivers James Njoroge, Reuben Ndolo and John Kaba, and field assistant Alex Kules; Lake Bogoria National Reserve staff, Jackson Komen and William Kimsop; and Dan Morton for his comments which helped to improve the manuscript. NASA Landsat imagery was provided by USGS. The work was carried out under research permission from the Kenyan Government's National Commission for Science, Technology & Innovation NCST/RCD/12B/013/21. Access and work at Bogoria had the permission of Baringo County Council's Chief Game Warden the Lake Bogoria National Reserve's Senior Warden; at Nakuru the permission of Kenya Wildlife Services. Permission to work at Lake Natron was granted by the Tanzanian Wildlife Research Institute, the Wildlife Division and the South Rift Association of Land Owners (SORALO).

Appendix A. Decision tree

See Fig. A.1.

References

Brezonik, P., Menken, K.D., Bauer, M., 2005. Landsat-based remote sensing of lake water quality characteristics, including chlorophyll and colored dissolved organic matter (CDOM). Lake Reserv. Manag. 21 (4), 373–382.

Brown, L., 1971. The breeding behaviour of the lesser flamingo Phoeniconaias minor. Ibis 113 (2), 147–172.

Castanier, S., Bernet-Rollande, M.-C., Maurin, A., Perthuisot, J.-P.,1993. Effects of microbial activity on the hydrochemistry and sedimentology of Lake Logipi, Kenya. In: Saline Lakes V: Proceedings of the Vth International Symposium on Inland Saline Lakes, held in Bolivia. 22–29 March 1991. Vol. 87 of Developments in Hydroiology. Springer, pp. 99–112.

Chander, G., Markham, B.L., Helder, D.L., 2009. Summary of current radiometric calibration coefficients for Landsat MSS, TM, ETM+, and EO-1 ALI sensors. Remote Sens. Environ. 113, 893–903, http://dx.doi.org/10.1016/j.rse.2009.01.007

Chavez, P., 1988. An improved dark-object subtraction technique for atmospheric scattering correction of multispectral data. Remote Sens. Environ. 24 (3), 459–479.

Chavez, P., 1996. Image-based atmospheric corrections-revisited and improved. Photogramm. Eng. Remote Sens. 62 (9), 1025–1036.

Childress, B., Nagy, S., Hughes, B.C., 2008. International Single Species Action Plan for the Conservation of the Lesser Flamingo, *Phoeniconaias Minor*, CMS Technical Series No. 18, AEWA Technical Series No. 34, Bonn, Germany.

Dubelaar, G.B., Visser, J.W., Donze, M., 1987. Anomalous behaviour of forward and perpendicular light scattering of a cyanobacterium owing to intracellular gas vacuoles. Cytometry 8, 405–412, http://dx.doi.org/10.1002/cyto.990080410

Gitelson, A., 1992. The peak near 700 nm on radiance spectra of algae and water: relationships of its magnitude and position with chlorophyll concentration. Int. J. Remote Sens. 13 (17), 3367–3373.

Harper, D., Mwinami, T., 2006. Thousands of lesser flamingos at Lake Naivasha? Kenya Birds 11, 11–15.

Harper, D.M., Childress, R.B., Harper, M.M., Boar, R.R., Hickley, P., Mills, S.C., 2003. Aquatic biodiversity in saline lakes: Lake Bogoria National Reserve, Kenya. Hydrobiologia 500, 259–276.

Irish, R., 2000. Landsat 7 Science Data Users Handbook. National Aeronautics and Space Administration, Report 430–15 http://landsathandbook.gsfc.nasa.gov/

Jerlov, N.G., 1976. Marine Optics, Vol. 14. Elsevier Science Limited.

Kaggwa, M., Gruber, M., Oduor, S., Schagerl, M., 2012. A detailed time series assessment of the diet of Lesser Flamingos: further explanation for their itinerant behaviour. Hydrobiologia, 1–11, http://dx.doi.org/10.1007/s10750-012-1105-1

Kirk, J.T., 1994. Light and Photosynthesis in Aquatic Ecosystems. Cambridge University Press, Cambridge, UK.

Kurekin, A., Miller, P., Van der Woerd, H., 2014. Satellite discrimination of Karenia mikimotoi and Phaeocystis harmful algal blooms in European coastal waters: merged classification of ocean colour data. Harmful Algae 31, 163–176.

Kutser, T., Vahtmäe, E., Metsamaa, L., 2006. Spectral library of macroalgae and benthic substrates in Estonian coastal waters. Proc. Estonian Acad. Sci. Biol. Ecol., 329–340.

Li, Y., Wang, Q., Wu, C., Zhao, S., Xu, X., Wang, Y., Huang, C., 2012. Estimation of chlorophyll a concentration using NIR/red bands of MERIS and classification procedure in inland turbid water. IEEE Trans. Geosci. Remote Sens. 50 (3), 988–997, http://dx.doi.org/10.1109/TGRS.2011.2163199

Liu, J., Sun, D., Zhang, Y., Li, Y., 2013. Pre-classification improves relationships between water clarity, light attenuation, and suspended particulates in turbid inland waters. Hydrobiologia 711 (1), 71–86.

Lobo, F.D.L., Novo, E.M.L.D.M., Barbosa, C.C.F., Galvão, L.S., 2012. Reference spectra to classify Amazon water types. Int. J. Remote Sens. 33 (11), 3422–3442.

Lugomela, C., Pratap, H.B., Mgaya, Y.D., 2006. Cyanobacteria blooms - A possible cause of mass mortality of Lesser Flamingos in Lake Manyara and Lake Big Momela, Tanzania. Harmful Algae 5, 534–541.

Matthews, M., Bernard, S., Robertson, L., 2012. An algorithm for detecting trophic status (chlorophyll-a), cyanobacterial-dominance, surface scums and floating vegetation in inland and coastal waters. Remote Sens. Environ. 124, 637–652.

Melack, J., 1988. Primary producer dynamics associated with evaporative concentration in a shallow, equatorial soda lake (Lake Elmenteita, Kenya). Hydrobiologia 158 (1), 1–14.

Morel, A., Prieur, L., 1977. Analysis of variations in ocean color. Limnol. Oceanogr. 22 (4).

Oberholster, P.J., Botha, A.-M., 2010. Use of remote sensing and molecular markers to detect toxic cyanobacterial hyperscum crust: a case study on Lake Hartbeespoort, South Africa. Afr. J. Biotechnol. 9 (51), 8791–8799.

Oduor, S., Schagerl, M., 2007a. Phytoplankton primary productivity characteristics in response to photosynthetically active radiation in three Kenyan Rift Valley saline-alkaline lakes. J. Plankton Res. 29 (12), 1041–1050.

Oduor, S.O., Schagerl, M., 2007b. Temporal trends of ion contents and nutrients in three Kenyan Rift Valley saline–alkaline lakes and their influence on phytoplankton biomass. Hydrobiologia 584, 59–68.

Robinson, I., Arthur, A.M., 2012. The FSF Post Processing Toolbox User Guide, Technical report.

Shi, K., Li, Y., Li, L., Lu, H., Song, K., Liu, Z., Xu, Y., Li, Z., 2013. Remote chlorophyll-a estimates for inland waters based on a cluster-based classification. Sci. Total Environ. 444, 1–15, http://dx.doi.org/10.1016/j.scitotenv.2012.11.058

Shi, W., Wang, M., 2009. An assessment of the black ocean pixel assumption for MODIS SWIR bands. Remote Sens. Environ. 113 (8), 1587–1597.

Smol, J.P., Stoermer, E.F. (Eds.), 2010. The Diatoms: Applications for the Environmental and Earth Sciences. Cambridge University Press.

Sun, D., Li, Y., Wang, Q., Le, C., Lv, H., Huang, C., Gong, S., 2012. Specific inherent optical quantities of complex turbid inland waters, from the perspective of water classification. Photochem. Photobiol. Sci. 11 (8), 1299–1312, http://dx.doi.org/10.1039/c2pp25061f

Talling, J., Driver, D.,1963. Some problems in the estimation of chlorophyll-a in phytoplankton. In: Proceedings of Conference of Primary Productivity Measurement, Marine and Freshwater. U.S. Atomic Energy Commission, Hawaii, pp. 142–146.

Tebbs, E., 2014. Remote sensing for the study of ecohydrology in East African Rift lakes. Ph.D. thesis. https://lra.le.ac.uk/handle/2381/28918?mode=full

Tebbs, E., Remedios, J., Avery, S., Harper, D., 2013. Remote sensing the hydrological variability of Tanzania's Lake Natron, a vital Lesser Flamingo breeding site under threat. Ecohydrol. Hydrobiol., http://dx.doi.org/10.1016/j.ecohyd.2013.02.002

Tebbs, E., Remedios, J., Harper, D., 2013b. Remote sensing of chlorophyll-a as a measure of cyanobacterial biomass in Lake Bogoria, a hypertrophic, saline-alkaline, flamingo lake, using Landsat ETM+. Remote Sens. Environ. 135, 92–106.

Tuite, C.H., 2000. The distribution and density of lesser flamingos in East Africa in relation to food availability and productivity. Waterbirds 23, 52–63.

Vareschi, E., 1978. The ecology of Lake Nakuru (Kenya). I. Abundance and feeding of the lesser flamingo. Oecologia 32 (1), 11–35.

Vincent, R.K., Qin, X., McKay, R.M.L., Miner, J., Czajkowskia, K., Savino, J., Bridgeman, T., 2004. Phycocyanin detection from LANDS, TM data for mapping cyanobacterial blooms in Lake Erie. Remote Sens. Environ. 89 (3), 381–392.

Xu, H., 2006. Modification of Normalised Difference Water Index (NDWI) to enhance open water features in remotely sensed imagery. Int. J. Remote Sens. 27 (14), 3025–3033.